

Article

Not peer-reviewed version

---

# Postfilament-Induced Two-Photon Fluorescence of Dyed Liquid Aerosol Enhanced by Structured Femtosecond Laser Pulse

---

D V Apeksimov, [P. A. Babushkin](#), [Yury E. Geints](#)\*, A. M. Kabanov, E. E. Khoroshaeva, [V. K. Oshlakov](#), A. V. Petrov, [Aleksandr A. Zemlyanov](#)

Posted Date: 3 June 2024

doi: [10.20944/preprints202406.0061.v1](https://doi.org/10.20944/preprints202406.0061.v1)

Keywords: femtosecond laser pulse; turbulence; aerosol; atmosphere; fluorescence; filamentation



Preprints.org is a free multidiscipline platform providing preprint service that is dedicated to making early versions of research outputs permanently available and citable. Preprints posted at Preprints.org appear in Web of Science, Crossref, Google Scholar, Scilit, Europe PMC.

Copyright: This is an open access article distributed under the Creative Commons Attribution License which permits unrestricted use, distribution, and reproduction in any medium, provided the original work is properly cited.

Disclaimer/Publisher's Note: The statements, opinions, and data contained in all publications are solely those of the individual author(s) and contributor(s) and not of MDPI and/or the editor(s). MDPI and/or the editor(s) disclaim responsibility for any injury to people or property resulting from any ideas, methods, instructions, or products referred to in the content.

## Article

# Postfilament-Induced Two-Photon Fluorescence of Dyed Liquid Aerosol Enhanced by Structured Femtosecond Laser Pulse

D.V. Apeksimov, P.A. Babushkin, Yu.E. Geints <sup>\*</sup>, A.M. Kabanov, E.E. Khoroshaeva, V.K. Oshlakov, A.V. Petrov and A.A. Zemlyanov

V.E. Zuev Institute of Atmospheric Optics of Siberian Branch of the Russian Academy of Science, 1, Academician Zuev Square, Tomsk, 634055, Russia

<sup>\*</sup> Correspondence: author: ygeints@iao.ru

**Abstract:** Laser-induced fluorescence spectroscopy (LIFS) is actively used for remote sensing of atmospheric aerosols and currently is one of the most sensitive and selective techniques for determining small concentrations of substances inside particles. The use of high-power femtosecond laser sources for LIFS-based remote sensing of aerosol contributes to the development of new-generation fluorescence atmospheric lidars since it makes it possible overcoming the energy threshold for the nonlinear-optical effects of multiphoton absorption in particles and receiving the emission signal at long distances in the atmosphere. Our study is aimed to the development and experimental demonstration the technique of nonlinear laser-induced fluorescence spectroscopy (NLIFS) based on the remote excitation of aerosol fluorescent emission stimulated by a spatially-structured high-power femtosecond laser pulse. Importantly, for the first time to our knowledge, we demonstrate the advances of using stochastically-structured plasma-free intense light channels (postfilaments) specially formed by propagation of femtosecond laser radiation through a turbulent air layer for improving NLIFS efficiency. A multiple increase in the received signal of two-photon-excited fluorescence of polydisperse dyed aqueous aerosol by the structured postfilaments is reported.

**Keywords:** femtosecond laser pulse; turbulence; aerosol; two-photon-excited fluorescence; angular distribution

---

## 1. Introduction

Femtosecond laser-induced fluorescence spectroscopy (FLIFS) and femtosecond laser-induced optical breakdown spectroscopy (FLIBS) are important tools for remote diagnostics of atmospheric aerosols using the LiDAR techniques. High intensity values inherent to the ultrashort optical radiation allow for overcoming the energy threshold for the realization of nonlinear-optical effects of multiphoton absorption and optical breakdown of matter inside the particles and provide for the receiving the emission signal from particles at long distances in the atmosphere via the lidars [1–7]. At sufficiently high laser intensity, a dyed liquid particle exposed to an optical radiation can be multiphoton-excited and exhibiting nonlinear emission in the spectral band of dye fluorescence. For example, for a typical laser dye (fluorescein-uranine,  $C_{20}H_{12}O_5$ ) the center of the broad spectral fluorescence band is located near the wavelength  $\lambda = 525$  nm, while the absorption band center is located around 500 nm. Obviously, since the energy of the near infra-red (IR) laser radiation quantum (carrier wavelength 800 nm) is less than the energy difference of the absorption levels of the dye molecule, the two-photon-excited fluorescence (TPEF) of the main energy transition of uranine is possible. As a result of TPEF, two quanta of incident radiation are absorbed by the dye molecule in one quantum event (one-step) and then the lower excited vibrational sublevel is released through the radiative transition to the ground singlet state.

The fluorescence arising in the droplet, which can be treated as the secondary radiation, is emerged mainly in the vicinity of the internal optical focuses, the so-called "hot spots" [8,9]. During

the propagation away from the hot spots this secondary radiation experiences refraction on the internal spherical surface of the mother particle. This results in a nonhomogeneous spatial distribution of the TPEF far from the particle (the receiving plane). On the other hand, the specific type of the angular distribution of dye emission is also influenced by the very nature of the excitation of secondary radiation, namely, by the multiphoton order ( $m$ ) of the excitation. In Ref. [8], multiphoton-excited fluorescence (two- and three-photon) angular patterns in ethanol and methanol droplets with 25–40  $\mu\text{m}$  radius containing coumarin 510 or tryptophan dyes are experimentally and theoretically investigated under the irradiation of a IR femtosecond Ti:Sapphire laser with typical pulse energy of several microjoules. The main result reported in this work is that the maximal intensity of droplets fluorescence is observed in the backward direction, i.e. towards the direction of incidence of the excitation radiation.

In our previous work [9], by means of the numerical FDTD simulation we showed that the higher the values of the  $m$ -photon order the more narrow-directed the radiation pattern of nonlinear emission from particles becomes. Meanwhile, emission from sufficiently large droplets with the sizes  $d \gg \lambda$  is always characterized by anomalously enhanced backward luminescence.

Worthwhile noting, the method of light-induced fluorescence stimulated by the femtosecond laser radiation is not yet sufficiently developed for using on the long-range atmospheric links [7]. Primarily, this is due to the challenges of controlling the nonlinear propagation of a high-power laser pulse at long distances because of manifestation of the filamentation phenomenon [10]. The spatial position of the filamentation region is known to be considerably sensitive to the laser pulse power, beam quality, phase modulation, optical polarization etc. [11]. Here, as a prospective opportunity for remote optical sensing of the atmosphere one can propose the specific ultra-broadband laser radiation in the form of the, so-called, post-filamentation light channels, which further will be referred as the postfilaments. These postfilaments, in fact, can be treated as the highly confined optical traces of the filaments [12,13]. Importantly, although high, the typical postfilament intensity is insufficient for medium ionization and creating a plasma in air. However, the postfilaments still possess high intensity (up to a hundred  $\text{GW/cm}^2$ ) causing their reduced angular divergence due to Kerr self-focusing [14] and are confidently registered at a length of several kilometers [15]. This eliminates the necessity for precise positioning of plasma region along the optical path to impact the test object, since the postfilaments extend over much longer ranges than the regular filaments, and one should only control the filamentation onset distance and not its length. Moreover, the impact of such a plasma-free postfilament formed during femtosecond pulse propagation in air on a denser object (solid target, aerosol) leads to plasma formation in this object itself [14] with the emission of spectral lines of detected substances. At the same time, we could not find any literature and experimental data on the remote fluorescence measurements from aerosols placed not in the filamentation region but in the region of plasma-free postfilaments propagation.

In present work, we experimentally demonstrate the use the postfilaments formed during the femtosecond laser pulse filamentation in air for realization the FLIFS method in a dyed liquid aerosol with different disperse compositions. Our study shows not only the possibility of remote detection of aerosol dye fluorescence spectra excited by the plasma-free light channels, but paves the way for increasing the efficiency of MPEF through the femtosecond pulse structuring via stochastic phase modulation by a heated air jet with random refractive index perturbations.

## 2. Results and Discussion

Experimental schematics on the remote recording of the fluorescence in aqueous aerosol droplets doped with the uranine dye (concentration, approx. 0.4 g/l) is presented in Figure 1. The droplet emission originates from a two-photon absorption and subsequent radiative relaxation of dye molecules exposed to GW-level femtosecond laser pulses produced by a Ti:Sapphire laser oscillator. Optionally, a laser pulse may experience specific modulation using a thin layer of heated turbulent air, which imposes stochastic phase modulation of the optical pulse when passing through it.

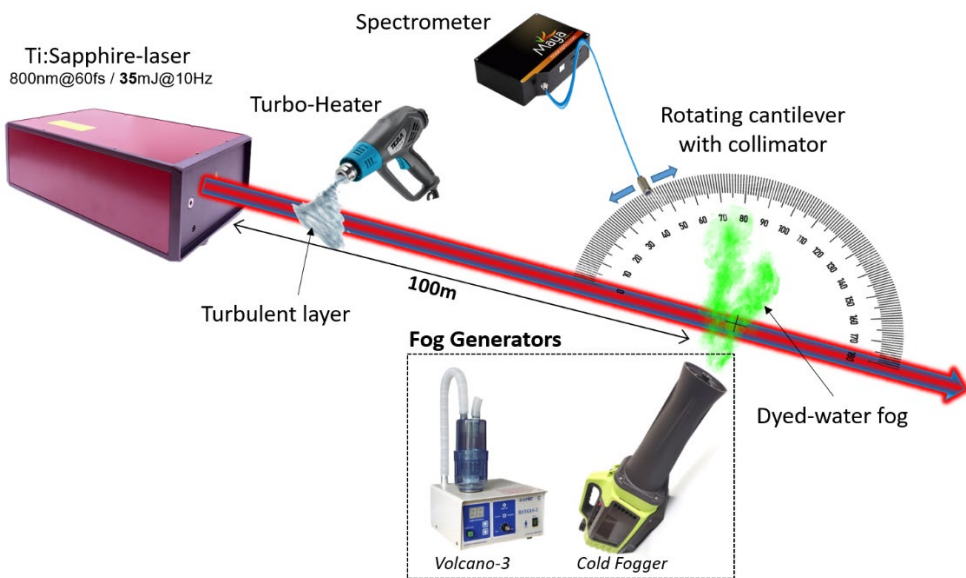


**Figure 1.** Experimental setup including Ti:Sapphire fs-laser, turbo-heater TESLA TH-2200 (temperature from 100 to 600°C), liquid aerosol (fog) generators Volcano-3 or Cold Fogger SF-720, receiving optical equipment (optical collimator, fiber, Maya-2000Pro spectrometer).

Recently [16], our experimental studies on the influence of turbulence on laser beam filamentation showed that the application of a thin but intense turbulent layer in the optical path of high-power laser radiation propagation leads to the intensity redistribution in the beam cross section due to the inhomogeneities of air refractive index, which initiates small-scale stochastic optical beam nucleation and the formation of high-intensity hot spots during the propagation. As an example, Figure 2a,b demonstrate the images of the transverse structure of a 35mJ femtosecond laser beam travelling a 100-m air path (a) without a turbulent layer and (b) when a turbo-heater is switched-on.

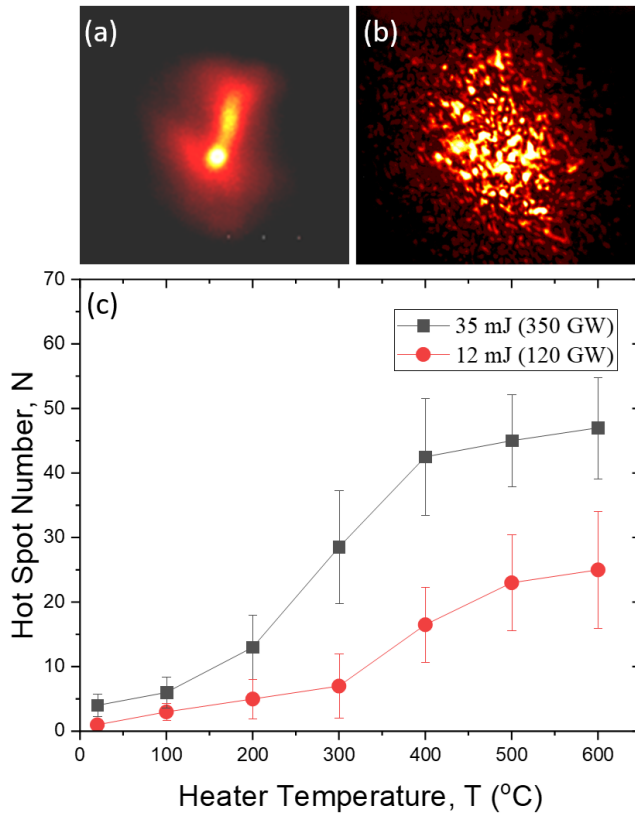


**Figure 2.** (a,b) Transverse beam fluence profile after 100-m air nonlinear propagation in (a) a calm atmosphere (without a turbulence) and (b) with a turbulent layer placed at the beginning ( $T = 400^{\circ}\text{C}$ ). (c) Number  $N$  of intensive hot spots (postfilaments) formed in a laser pulse after modulation by a turbulent jet produced at different heater temperature  $T$ .

For creation of a turbulent phase layer, our experimental setup provides for an air heating device with a variable temperature of the heating element. During our experiments, the air turbo-heater (fan) is placed at a distance of about 8 m from the laser output window at a lateral distance of 10 cm relative to the beam axis. The average thickness of the turbulent jet is about 2 cm. Figure 2(c) shows the number of intense post-filamentation channels formed in the laser beam as a function of the heater temperature for laser pulse with the energy of 12 and 35 mJ. As seen, both dependencies on the graph approach certain saturation level at the heater temperature  $T > 400^{\circ}\text{C}$ , which according to Figure 3f corresponds to air temperature  $T_{\text{air}}$  inside the optical beam of about  $160^{\circ}\text{C}$ . Worthwhile noting, after placing the turbulent layer in the optical path causes more than 10-fold increase in the number of intense postfilaments.

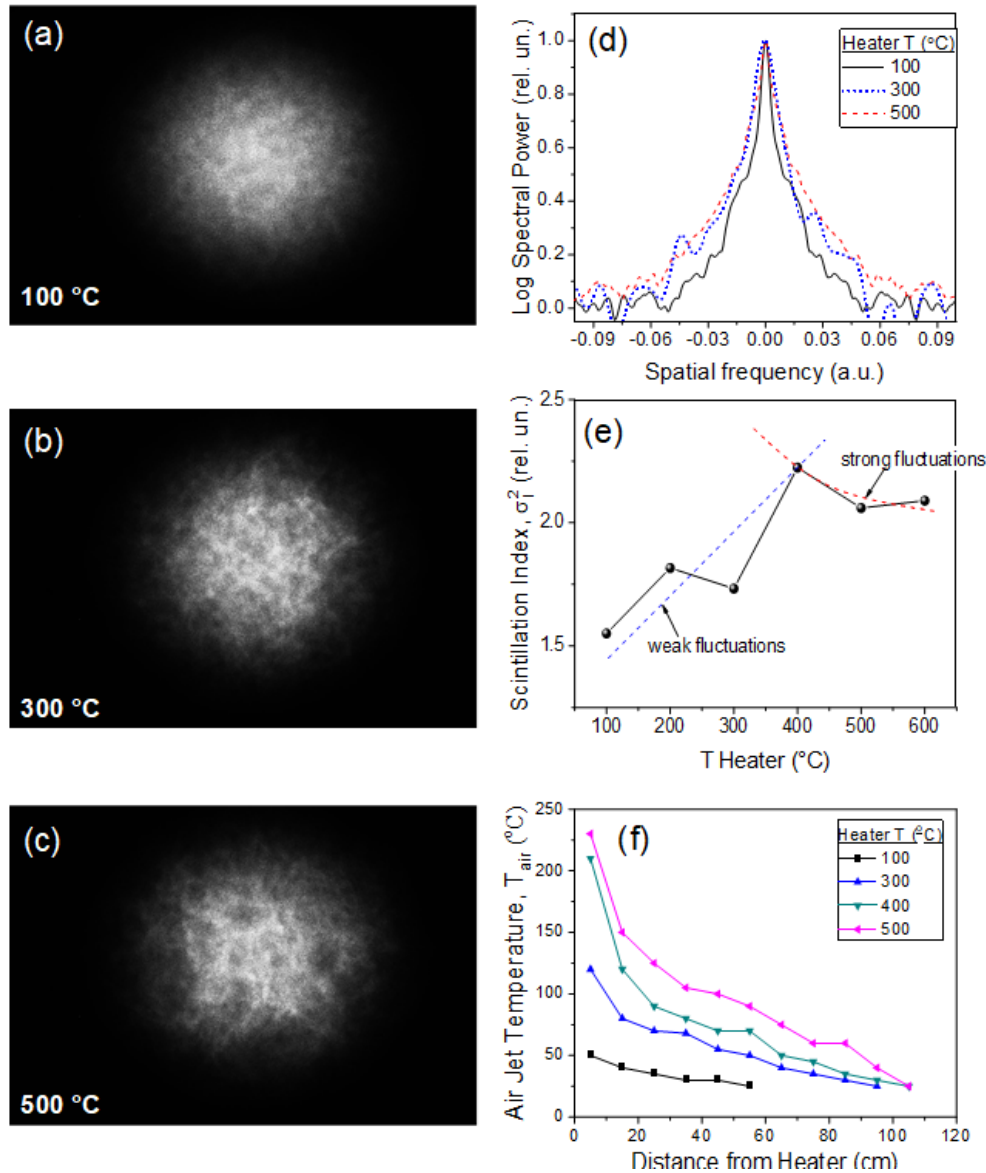
For the characterization of optical turbulence in this spatially-localized layer we calculate the turbulence structural function in the framework of the “2/3” law in the Kolmogorov-Obukhov statistical theory. In particular, the structural function, or more specifically the structural constant of the refractive index  $C_n^2$  can be measured from statistics of probe He-Ne laser beam (wavelength 630 nm) scintillation index  $\sigma_i^2$  (dispersion of intensity fluctuations) after the propagation through a turbulent layer considering the Kolmogorov or Karman spatial spectrum [17]. A standard measurement scheme is used including a photodetector and a point diaphragm (0.1 mm diameter aperture) aimed at the center of the laser beam with 2 Hz data accumulation rate. The information collected over a selected time interval (2 minutes) is then statistically averaged. The examples of probe beam speckle structure are shown in Figures 3a–c for different temperature regimes of the fan heater.

Figure 3(d) illustrates the power spectrum of the scintillation index  $\sigma_i^2$  measured in the central beam area. Obviously, a change in the heater temperature affects not only the temporal statistics of

the laser beam intensity pulsations, but also its spatial spectrum. In this figure, 1D intensity profiles (along the horizontal axis) are plotted after a test laser beam passes through a turbulent layer created at different heater temperatures. The intensity profiles shown in this figure are pre-processed using digital spatial filter for cutting-off the high-frequency noise components. It is clear that the amplitude of low-frequency perturbances increases sharply along with the fan temperature.

The data of  $\sigma_I^2$  time series statistical processing is summarized in Figure 3e. As seen, the normalized turbulent intensity pulsations first grow up to the value  $\sigma_I^2 \approx 2.25$  and then demonstrate a smooth decrease to  $\sigma_I^2 = 2.05$  with the increasing of the conditional air jet temperature  $T$ . The extremum of the scintillation index is observed for  $T = 400^\circ\text{C}$ . The character of the obtained dependence points to a certain analogy with the well-known result of Rytov theory for the behavior of the optical wave intensity dispersion in a random inhomogeneous medium [18]. According to this theory, two asymptotes can be distinguished in the dependence  $\sigma_I^2(C_n^2)$  corresponding to the regimes of a weak,  $\sigma_I^2 \propto C_n^2(T)$ , and strong turbulence:  $\sigma_I^2 \propto 1 + [C_n^2(T)]^{-4/5}$ .

These asymptotes are plotted in Fig. 3(e) by dashed lines and are calculated through the least-squares fitting procedure of the measurement data. This allows one to estimate the conditional range of  $C_n^2$ -values, within which the turbulence strength of the fan air jet could change when switching the heater temperature regimes. It turned out that the thermal regimes switching from  $100^\circ\text{C}$  to  $600^\circ\text{C}$  conditionally corresponds to the change of structural turbulence constant in the range of  $7 \cdot 10^{-9} \text{ m}^{-2/3} \leq C_n^2 \leq 3 \cdot 10^{-7} \text{ m}^{-2/3}$ . As expected, these values are close to those given in previous similar studies on the femtosecond pulses filamentation [17,19], but at the same time they are significantly higher than the typical values of atmospheric turbulence, where, as a rule,  $C_n^2 \leq 10^{-10} \text{ m}^{-2/3}$ .



**Figure 3.** Turbulence layer optical characterization. (a–c) Transverse profile of a probe He-Ne laser passed the turbulent layer at three heater temperatures  $T$ . (d) Beam power spectrum. (e) Scintillation index mean value versus heater temperature. (f) Air temperature  $T_{air}$  in turbulent layer depending on the distance from the heater measured by an IR-camera.

In the experimental measurements, a fine-dispersed water fog with modal particle diameter  $d \approx 12 \mu\text{m}$  is produced by the ultrasonic generator Volcano-3. The particle size distribution measured by the optical dust sensor (Alphasense OPC-N3) is presented in Figure 4. Effective particle concentration  $n$  in a fog is estimated from the measurements of aerosol transparency at the wavelength of a low-power CW He-Ne laser ( $\lambda = 632 \text{ nm}$ ) in the approximation of droplet monodisperse distribution. For this type of water aerosol, the particle concentration is approximately,  $n \approx 10^4 \text{ cm}^{-3}$ .

Another type of liquid aerosol used, a coarse aerosol with modal particle diameter  $d = 40$  or  $60 \mu\text{m}$  (see Figure 4a), is created by an atomizing aerosol generator (Cold Fogger SF-720) equipped with two nozzles, respectively. To measure the size distribution of particles, they are deposited on a transparent slide with an oil layer and processed using the software of a digital microscope "Mikmed-6 LOMO". A magnified image of the deposited aerosol is exemplified in Figure 4b. The images in

Figure 4c,d show fine- and coarse-dispersed aerosols luminescence in visible excited by an IR femtosecond laser pulse spatially modulated by a turbulent layer.

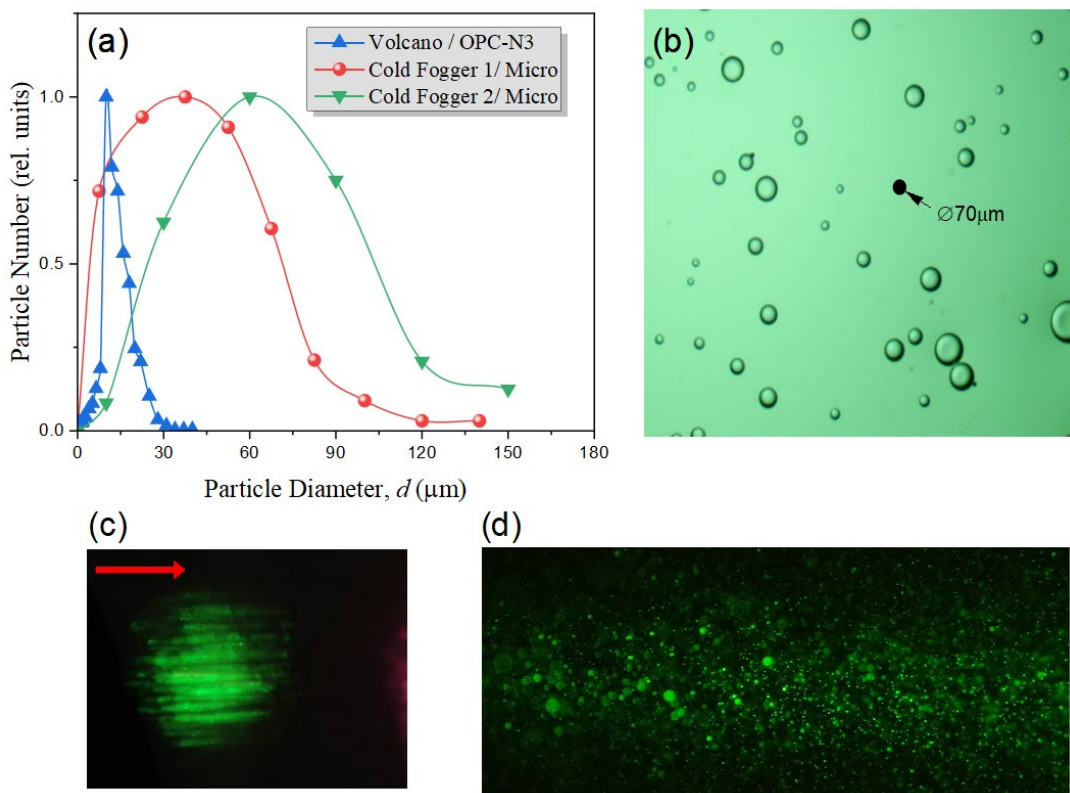


**Figure 4.** (a) Aerosol particle size distribution produced by Volcano-3 and Cold Fogger fog generators. (b) Magnified image of coarse water aerosol particles in immersion oil. (c,d) TPEF images of the fine-dispersed (c) and coarse-dispersed (d) aerosol. Ti:Sapphire laser pulse incidence is indicated by red arrow.

These images show green luminescence of dyed aerosol particles when irradiated with near-infrared radiation after the nonlinear propagation of 100 m in air. Besides, the two-photon fluorescence of aerosol is realized mainly in the form of intense channels which are formed within femtosecond IR beam cross-section.

Dyed aerosol fluorescence spectra are presented in Figure 5a,b for the cases with and without pulse turbulence modulation. Obviously, the installation of a turbulent layer in the optical path of femtosecond laser pulse causes spatial beam structuring and leads to an increase in the fluorescence intensity of droplets. This is because the spatially structured optical radiation produces significantly more hot spots that almost fully populate the beam cross-section with numerous light channels interacting with the aerosol jet. Due to this dense postfilament filling, the aerosol volume produces a more intensive fluorescence compared to a conventional Gaussian-profiled beam (i.e., without a turbulence modulation) which generates only few postfilaments (see, Figure 2a). The degree of nonlinear aerosol emission enhancement due to turbulence in the laser beam at the central wavelength, 520 nm, of uranine fluorescence band is approximately 20% for fine-dispersed aerosol and 30% for larger particles. This circumstance opens prospects for increasing the sensitivity and selectivity of methods for determining small concentrations of substances by femtosecond fluorescence spectroscopy using specially structured laser radiation.

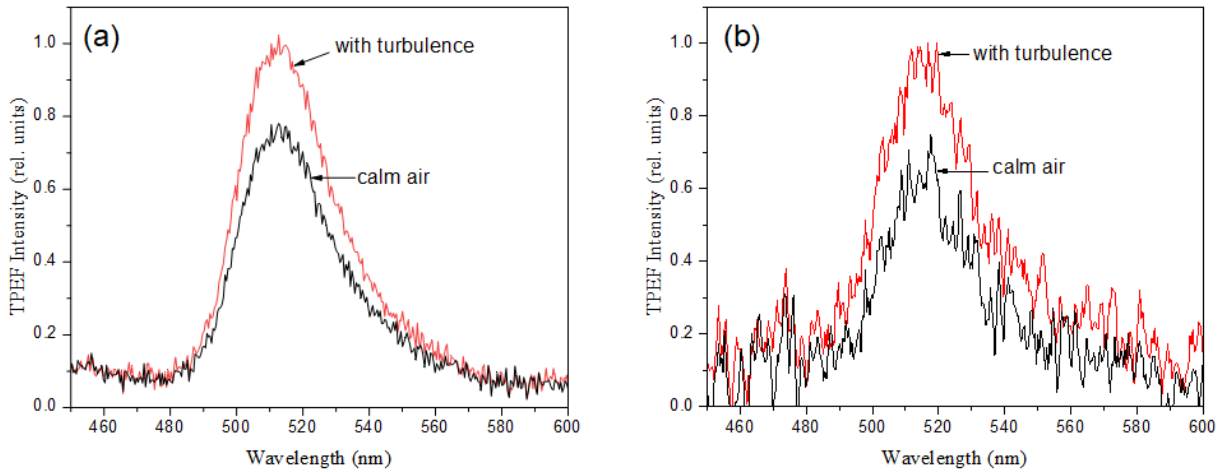


**Figure 5.** TPEF spectra of uranine-dyed water aerosol with/without turbulence modulation of femtosecond IR pulse for (a) fine and (b) coarse aerosol distribution (Cold Fogger 1&2 in Figure 4a).

The angular distribution of fluorescence from dyed aqueous droplets is shown in Figure 6a,b. This data is obtained by the spectral accumulation of aerosol droplet emission for each receiving direction in the whole spectral range of measurements. As seen, in general, TPEF angle distribution exhibits a quasi-dipole shape with a minimum intensity in the transverse direction, i.e., along the polarization of incident IR optical radiation, and with pronounced asymmetry in the forward-backward directions. The maximum of the two-photon droplet emission is observed in the angular range from approximately 160 to 170 degrees relative to the direction of femtosecond pulse exposure. The measured TPEF angular shape is characteristic both for the fine aerosol (Figure 6a) and coarse-dispersed particles (Figure 6b). The degree of forward-backward fluorescence asymmetry reaches about two times for fine-dispersed fog and almost three times for coarse-dispersed fog.

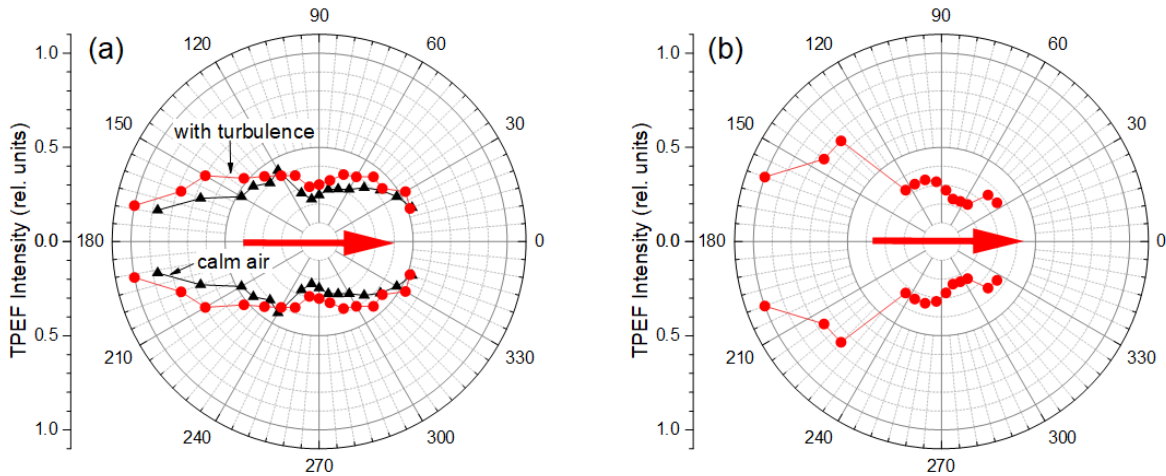


**Figure 6.** (a,b) TPEF angular distribution in dyed water aerosol with (a) fine and (b) coarse particle distribution stimulated by a femtosecond IR laser pulse passed through a thin turbulent layer. The data is averaged over 10 seconds.

It is worth noting that the dimensionless Mie parameter ( $Q = \pi d/\lambda$ ) for majority of particles in the distributions considered (Figure 4a) corresponds to the criterion of an optically large particle ( $Q \gg 1$ ) at the wavelength of the incident radiation  $\lambda = 800$  nm, which in the case of elastic optical scattering should lead to a sharp asymmetry of the scattered field with the predominance of forward Mie-scattering. Indeed, our theoretical simulation of Mie-scattering and nonlinear fluorescence of aqueous

particles shown in Figure 7a,b clearly demonstrates fundamental differences in the angular distribution of elastic scattering and the nonlinear TPEF process in dyed water droplets.

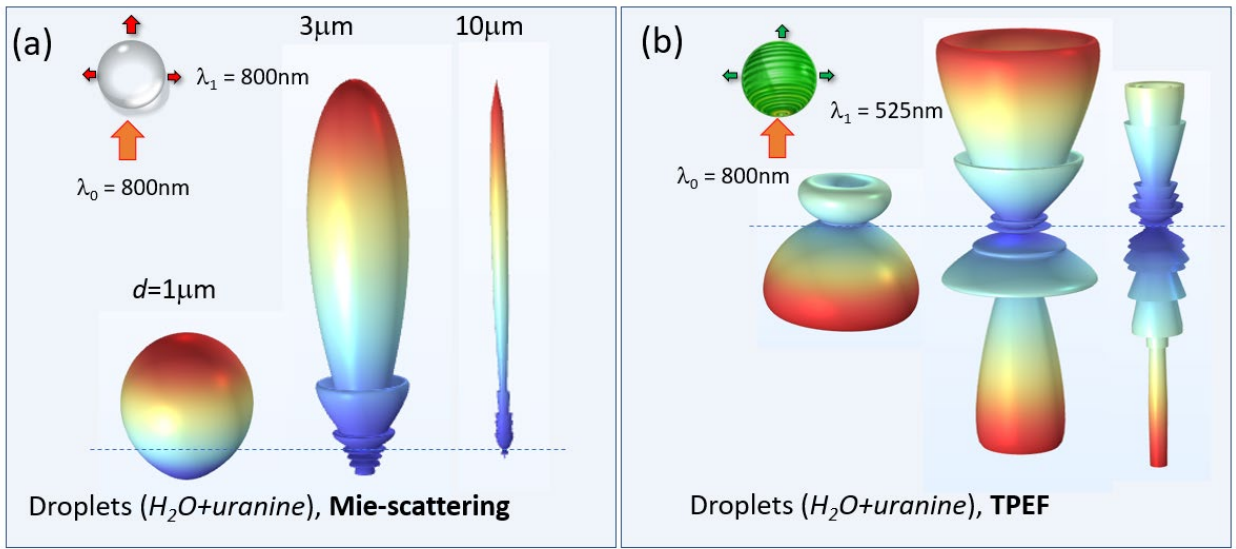


**Figure 7.** Simulated angular distribution of far-field scattered optical intensity from dyed water droplets of different radii. (a) elastic Mie-scattering and (b) two-photon fluorescence of uranine.

Theoretical simulation of the nonlinear droplet emission is based on the numerical solution of the Equation (1) by means of the finite element method implemented in the COMSOL Multiphysics software package. Since the emission of photons by a molecule/ion occurs spontaneously, in the numerical model the emitting dipoles at each point of particle generally are not correlated either in phase or in the direction.

During the simulation of spontaneous emission from a spherical particle within the stationary problem formulation, it is assumed that each molecule of matter inside the liquid particle behaves as a dipole that first absorbs some energy fraction of optical field  $\mathbf{E}_i(\mathbf{r})$  incident on the aerosol particle at the wavelength  $\lambda_0$  and then spontaneously emits a quantum of light at the shifted wavelength  $\lambda_1$ . Clearly, by neglecting the non-radiative relaxation mechanisms, the rate  $\gamma_d$  of spontaneous emission of a dipole (dipole transition probability) is proportional to the scalar product of the dipole moment of the corresponding transition  $\mathbf{p}_d$  and the local field strength  $\mathbf{E}_i$  raise to power  $m$ :

$$\gamma_d^{(m)} \propto \left| \mathbf{p}_d \cdot [\mathbf{E}_i(\mathbf{r})]^m \right|^2, \text{ where } m \text{ is the number of simultaneously absorbed optical field quanta.}$$

Following the considerations of Ref. [20], the equation describing the spontaneous fluorescence from a spherical particle is the inhomogeneous Helmholtz equation which is solved within the stationary problem formulation:

$$\left( k_0^2 \varepsilon_1 \right)^{-1} \nabla \times (\nabla \times \mathbf{E}_1(\mathbf{r})) - \mathbf{E}_1(\mathbf{r}) = \mathbf{P}_1 \{ \mathbf{E}_i(\mathbf{r}); \tilde{\mathbf{r}}_1 \} \quad (1)$$

Here,  $k_0$  is the wave number in free space,  $\varepsilon_1$  is medium permittivity, and the polarization source  $\mathbf{P}_1$  depends randomly on the radiating dipole spatial position  $\tilde{\mathbf{r}}_1$ :

$$\mathbf{P}_1(\mathbf{r}; \tilde{\mathbf{r}}_1) \propto \mathbf{n}_r I_i^{m-1} (\tilde{\mathbf{n}}_d \cdot \mathbf{E}_i), \quad (2)$$

where we use the notation  $I_i = |\mathbf{E}_i|^2$  for the optical intensity,  $\mathbf{n}_r = \mathbf{r}/|\mathbf{r}|$ , and  $\tilde{\mathbf{n}}_d \equiv \mathbf{n}_d(\tilde{\mathbf{r}}_1)$  denotes a randomly-oriented unit vector of the dipole ( $\mathbf{p}_d = |\mathbf{p}_d| \mathbf{n}_d$ ). Obviously, the rate of energy exchange of the optical field with a dipole in a unit volume of matter for the case of two-photon absorption ( $m = 2$ ) depends on the square of the pumping intensity  $I_i$ :  $\gamma_d^{(2)} \propto |E_i|^4 = I_i^2$ .

In the simulations, the statistics on the droplet emission is gathered by setting different (usually a hundred variants) spatial distributions of dipole moments inside a particle having random dipole

moment directions  $\tilde{\mathbf{n}}_d$ . For each of these variants the solution of the problem (1)-(2) is carried out separately. All the calculation series are eventually averaged over the spatial coordinates and the resulting angular distribution of the nonlinear droplet emission is obtained in the far-field region by using Stratton-Chu integrals [21].

Recalling Figure 7, one can see that with increasing particle radius, the angular distribution of the Mie-scattering is noticeably elongated in the forward direction, i.e. toward the value of  $0^\circ$ , while in the case of TPEF the angular distribution, on the contrary, deforms in the opposite direction, i.e. has a maximum in the direction toward the laser incidence as in the experiments. Interestingly, in the transverse direction both types of optical droplet emission show a decrease in intensity.

### 3. Conclusions

In this paper, we present the results of the laboratory experiments on remote detection of fluorescence spectra from uranine-dyed water aerosol with different size distribution exposed to high-intense optical channels formed during the nonlinear propagation of a femtosecond Ti:Sapphire laser pulse through a thin turbulent air layer. Our studies show that this stochastic fragmentation of high-power laser radiation, due to the development of small-scale self-focusing, leads to the formation of many high-intensity weakly diverging light channels (postfilaments) in the beam. The characteristic intensity of these postfilaments is sufficient for the realization of two-photon absorption of dye molecules in the volume of aerosol particles, which in turn significantly increases the magnitude of the fluorescence signal received. The measured values of the angular directivity of nonlinear emission of particles indicate the appearance of a pronounced asymmetry in the angular distribution of aerosol fluorescence in the back hemisphere and an insignificant influence of particle dispersity on the angular directivity of optical excitation of dye molecules by incident optical radiation. This circumstance opens prospects for increasing the sensitivity and selectivity of methods for determining small concentrations of substances by femtosecond fluorescence spectroscopy using specially structured laser radiation.

**Funding:** Ministry of Science and Higher Education of Russian Federation; Russian Science Foundation (No. 24-12-00056).

**Data Availability.** Data underlying the results presented in this paper are not publicly available at this time but may be obtained from the authors upon reasonable request.

**Disclosures.** The authors declare no conflicts of interest.

### References

1. Kasparian, J.; Rodriguez, M.; Mejean, G.; Yu, J.; Salmon, E.; Wille, H.; Bourayou, R.; Frey, S.; Andre, Y.-B.; Mysyrowicz, A.; Sauerbrey, R.; Wolf, J.-P.; Woeste, L. "White-light filaments for atmospheric analysis," *Science* 301, 61-64 (2003): <https://doi.org/10.1126/science.1085020>.
2. H. L. Xu, W. Liu, and S. L. Chin, "Remote time-resolved filament-induced breakdown spectroscopy of biological materials," *Opt. Lett.* 31(10), 1540–1542 (2006): <https://doi.org/10.1364/OL.31.001540>.
3. J. F. Daigle, G. Méjean, W. Liu, F. Théberge, H. L. Xu, Y. Kamali, J. Bernhardt, A. Azarm, Q. Sun, P. Mathieu, G. Roy, J. R. Simard, and S. L. Chin, "Long range trace detection in aqueous aerosol using remote filament-induced breakdown spectroscopy," *Appl. Phys. B* 87(4), 749–754 (2007): <https://doi.org/10.1007/s00340-007-2642-6>.
4. Y. Kamali, J.-F. Daigle, F. Theberge, M. Chbteauneuf, A. Azarm, Y. Chen, C. Marceau, S.C. Lessard, F. Lessard, G. Roy, J. Dubois, S.L. Chin, "Remote sensing of trace methane using mobile femtosecond laser system of T&T Lab," *Opt. Commun.* 282, 2062–2065. (2009).
5. S.S. Golik, A.Y. Mayor, V.V. Lisitsa, Y.S. Tolstonogova, A.A. Ilyin, A.V. Borovskiy, and O.A. Bukin, "Limits of Detection of Chemical Elements in an Aqueous Aerosol in Filament-Induced Breakdown Spectroscopy," *J. Appl. Spectrosc.* 88(2), 337–342 (2021): <https://doi.org/10.1007/s10812-021-01179-3>.
6. P.A. Babushkin, G.G. Matvienko, and V.K. Oshlakov, "Determination of the elemental composition of aerosol by femtosecond laser-induced breakdown spectroscopy," *Atmospheric and Oceanic Optics* 35(1), 19–26 (2022); <https://doi.org/10.1134/S102485602201002X>.

7. D.V. Apeksimov, Yu.E. Geints, V.K. Oshlakov, and A.V. Petrov, "Experimental demonstration of dyed water aerosol fluorescence stimulated by femtosecond laser postfilaments propagating in air," *Appl. Opt.* 62, 6401-6406 (2023).
8. Boutou, V.; Favre, C.; Hill, S.C.; Pan, Y.-L.; Chang, R.K.; Wolf, J.-P. "Backward enhanced emission from multiphoton processes in aerosols," *Appl. Phys. B* 75, 145-152 (2002): <https://doi.org/10.1007/s00340-002-0970-0>.
9. Yu. E. Geints, A. A. Zemlyanov, and E. K. Panina, "Modeling of Multiphoton Excited Fluorescence from a Spherical Droplet Irradiated by an Ultrashort Laser Radiation Using the Method of Computation Electrodynamics," *Atmospheric and oceanic optics* 24, 294 (2011): <https://doi.org/10.1134/S1024856011030079>.
10. R.W. Boyd, S.G. Lukishova, Y.R. Shen, *Self-focusing: Past and present. Fundamentals and prospects* (Springer, 2009).
11. S. V. Chekalin, V. P. Kandidov, "From self-focusing light beams to femtosecond laser pulse filamentation," *Physics-Uspekhi*, 56(2), 123-140 (2013). <https://doi.org/10.3367/UFNe.0183.201302b.0133>.
12. G. Méchain, A. Couairon, Y.-B. André, C. D'Amico, M. Franco, B. Prade, S. Tzortzakis, A. Mysyrowicz and R. Sauerbrey, "Long-range self-channeling of infrared laser pulses in air: A new propagation regime without ionization," *Appl. Phys. B* 79, 379 (2004).
13. J.-F. Daigle, O. Kosareva, N. Panov, T.-J. Wang, S. Hosseini, S. Yuan, G. Roy, S.L. Chin "Formation and evolution of intense, post-filamentation, ionization-free low divergence beams," *Opt. Commun.* 284, 3601-3606 (2011).
14. D.V. Apeksimov, A.A Zemlyanov, A.M. Kabanov, A.N. Stepanov, "Postfilamentation light channels in the air," *Atmospheric and oceanic optics* 30, 451-455 (2017): <https://doi.org/10.1134/S1024856017050025>.
15. Durand M., Houard A., Prade B., Mysyrowicz A., Durécu A., Moreau B., Fleury D., Vasseur O., Borchert H., Diener K., Schmitt R., Théberge F., Chateauneuf M., Daigle J.-F., Dubois J. Kilometer range filamentation // *Opt. Express.* 2013. V. 21. P. 26836-26845.
16. D.V. Apeksimov, A.V. Bulygin, Yu.E. Geints, A.M. Kabanov, E.E. Khoroshaeva, A.V. Petrov, V.K. Oshlakov, "Statistical parameters of femtosecond laser pulse post-filament propagation on 65m air path with localized optical turbulence," *J. Opt. Soc. Am. B* 39, 3237-3246 (2022): <https://doi.org/10.1364/JOSAB.473298>.
17. R. Ackermann, G. Méjean, J. Kasparian, J. Yu, E. Salmon, J.-P. Wolf, "Laser filaments generated and transmitted in highly turbulent air," *Opt. Lett.* 31, 86 (2006): <https://doi.org/10.1364/OL.31.000086>.
18. V.O. Kompanets, S.V.Chekalin, O.G.Kosareva, A.V. Grigor'evskii, V.P. Kandidov, "Conical emission of a femtosecond laser pulse focused by an axicon into a K 108 glass", *Quantum Electron.* 36 (9), 821 (2006): <https://doi.org/10.1070/QE2006v036n09ABEH013195>.
19. R. Salame, N. Lascoux, E. Salmon, R. Ackermann, and J. Kasparian, "Propagation of laser filaments through an extended turbulent region," *Appl. Phys. Lett.* 91, 171106 (2007): <https://doi.org/10.1063/1.2799163>.
20. Yu. E. Geints, "Angular Patterns of Nonlinear Emission in Dye Water Droplets Stimulated by a Femtosecond Laser Pulse for LiDAR Applications," *Remote Sens.* 15, 4004 (2023): <https://doi.org/10.3390/rs15164004>.
21. M.S. Zhdanov Stratton-Chu Type Integrals. In: *Integral Transforms in Geophysics*. Springer, Berlin, Heidelberg (1988). [https://doi.org/10.1007/978-3-642-72628-6\\_8](https://doi.org/10.1007/978-3-642-72628-6_8).

**Disclaimer/Publisher's Note:** The statements, opinions and data contained in all publications are solely those of the individual author(s) and contributor(s) and not of MDPI and/or the editor(s). MDPI and/or the editor(s) disclaim responsibility for any injury to people or property resulting from any ideas, methods, instructions or products referred to in the content.